Quantifying Exciton Transport in Singlet Fission Diblock Copolymers

Guiying He[1,2†], Lauren M. Yablon[3†], Kaia R. Parenti[3], Kealan J. Fallon[3], Luis M. Campos[3*], Matthew Y. Sfeir[1,2*]

[1]Department of Physics, Graduate Center, City University of New York, New York, NY 10016, USA

[2]Photonics Initiative, Advanced Science Research Center, City University of New York, New York, NY 10031, USA

[3]Department of Chemistry, Columbia University, New York, New York 10027, USA

[†]Contributed equally to this work.

* lcampos@columbia.edu

* msfeir@gc.cuny.edu

Abstract

Singlet fission (SF) is a mechanism of exciton multiplication in organic chromophores, which has potential to drive highly efficient optoelectronic devices. Creating effective device architectures that operate by SF critically depend on electronic interactions across multiple length scales – from individual molecules, to interchromophore interactions that facilitate multiexciton dephasing, and exciton diffusion toward donor-acceptor interfaces. Therefore, it is imperative to understand the underpinnings of multiexciton transport and interfacial energy transfer in multichromophore systems. Interestingly, block copolymers (BCPs) can be designed to control multiscale interactions by tailoring the nature of the building blocks, yet SF dynamics are not well understood in these macromolecules. Here, we designed diblock copolymers comprising an inherent energy cleft at the interface between a block with pendent pentacene chromophores and an additional block with pendent tetracene chromophores. The singlet and triplet energy offset between the two blocks creates a driving force for exciton transport along the BCP chain in dilute solution. Using time-resolved optical spectroscopy, we have quantified yields of key energy transfer steps, including both singlet and triplet energy transfer processes across the pentacene-tetracene interface. From this modular BCP architecture, we correlate the energy transfer timescales and relative yields with the length of each block. The ability to quantify these energy transfer processes provides valuable

insights into exciton transport at critical length scales between bulk crystalline systems and small molecule dimers – an area that has been under explored.

Introduction

Multiexciton processes in organic systems have generated interest due to their potential to bolster the performance of optoelectronic devices.[1–5] Importantly, the ability to understand how to generate and control the fate of multiexcitons in organic materials could lead to transformative technologies and fundamental knowledge. Organic chromophores that undergo singlet fission, a process that converts one high energy singlet exciton (S_1) into two lower energy triplet excitons ($2\times T_1$) via a correlated triplet pair (TT), are particularly interesting because they can yield triplet excitons with lifetimes in the microsecond regime.[6–8] The long lifetime of the triplets can enable efficient exciton harvesting at donor-acceptor heterojunctions.[9–11] In fact, enhanced photocurrents have been observed in a number of singlet fission sensitized semiconductor devices.[11–14] However, in each of these architectures, triplet harvesting occurred primarily at the organic-semiconductor interface, requiring extremely thin active layers with limited optical absorption. Further improvement in multiexciton harvesting schemes will require more efficient extraction of triplet pairs generated at larger distances from an interface. However, there is a gap of knowledge in understanding intramolecular exciton diffusion[15–17] and exciton transfer in key singlet fission systems.[18–20] This requires new fundamental insights into the nature of interfacial interactions and the role of molecular engineering in tuning the triplet dynamics, which can inform device engineering for optimal performance.

The mechanism of singlet fission has been generally studied in crystals of individual chromophores and in dilute solution, using small molecule dimers and short oligomers.[21,22] In the condensed phase, crystalline small molecules undergo intermolecular singlet fission (xSF) enabled by through-space coupling interactions, resulting in mobile triplets whose lifetime depends strongly on the rigid crystal structure, grain size and defect density.[23,24] Furthermore, heterochromophore singlet fission (HSF) has been observed at the two extreme length scales – small molecule dimers (Figure 1a)[25,26] and bulk, solid-state heterogeneous blends of pentacene and tetracene (Figure 1b).[27] Diffusion in solid-state systems can be readily quantified using real space imaging, polarization dependent studies, or by measuring population dynamics as a function of changes in the material's property.[28–30] At the other limit in dilute solution, covalently linked heterochromophore molecules exhibit intramolecular singlet fission (iHSF) enabled by through-

bond/space interactions.[31–34] In these systems, connectivity of the chromophores plays a crucial role in the excited state dynamics. Guided by structure-property relationships, iHSF systems have been designed to yield free triplets with long lifetimes.[6,8,24,35–37] However, exciton diffusion is limited by the length of the oligomers and mediated by through-bond migration.[34]

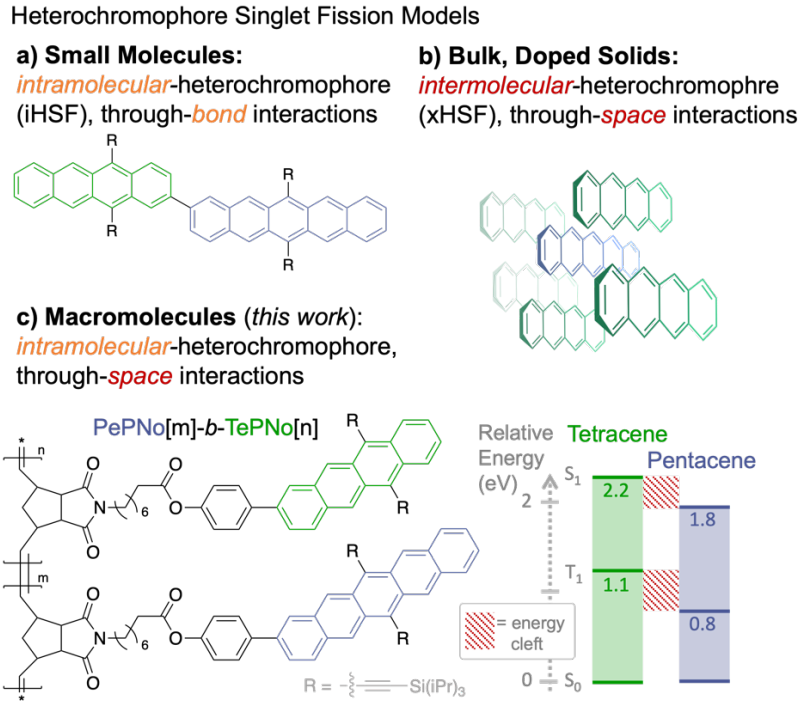

Figure 1. **a)** Small molecule dimer model that undergoes heterochromophore singlet fission enabled by through-bond interactions. **b)** Schematic representation of a pentacene-doped tetracene solid system that undergoes heterochromophore singlet fission mediated by through-space interactions between different molecules. **c)** Macromolecular model – chemical structure of the singlet fission diblock copolymer **PePNo[m]-*b*-TePNo[n]**, comprising an insulating polynorbornene backbone (PNo) with pendent pentacene (Pe) and tetracene (Te) moieties, where [m] and [n] represent the degree of polymerization (DP). The relative energies of the singlet (S_1) and triplet (T_1) states of the chromophores show the offset energy cleft. *Note: we adopted the term "heterochromophore" SF to accurately represent the differences between systems in **a/c** and **b** above, since "heteromolecular" SF implies a process between two different molecules (which is the case in **b**); but it is two different types of chromophores within only one (macro)molecule in both **a** and **c**.

Considering that small molecules and crystalline systems have been widely studied, less research has been conducted on the diffusion of triplet excitons produced by singlet fission in macromolecules, such as dendrimers and polymers.[38–45] Macromolecules can be engineered with precise control over the number and type of interchromophore interactions, while providing an extended framework for studying mobile triplet excitons. Rigid star macromolecules of pentacene (and tetracene) have been found to yield short-lived triplets (*TT*) due to the strong coupling between the chromophores by through-bond and through-space interactions.[46] However, pendent pentacene polymers exhibit fast rates of singlet fission by through-space interactions of the pendent chromophores, yielding mobile free triplet excitons ($2\times T_1$) that recombine via a secondary geminate process.[36] In contrast to conjugated iSF polymers that yield short-lived triplets,[39–41,43–45,47] pendent pentacene polymers can lead to the generation of remarkably long-lived triplets (microseconds). Interestingly, the pendent pentacene polymers have triplet lifetimes that depend on the length of the polymers until reaching saturation at a large number of repeat units. This, and neutron scattering characterization, suggests that the secondary structure and rigidity/flexibility of the polymer plays a crucial role in dictating diffusion lengths.[36] Considering the rich information of exciton diffusion from these polymers, we recognized that such architecture could be readily altered to obtain block copolymers (BCPs) with chromophores that provide directional exciton diffusion in the presence of an energy cleft.

Here, we leverage the architectural features of polymers with pendent chromophores (Figure 1c) to study interfacial interactions that other multichromophore systems with random molecule distributions and poorly defined interfaces between different molecules are simply not well suited for, e.g. amorphous blends and concentrated solution mixtures of individual chromophores (Figure 1c). Block copolymers are generally exploited for their ability to undergo phase segregation that can lead to ordering in the solid state and in solution, a property that can be implemented with SF chromophores to study multiexciton dynamics in ordered morphologies.[48–50] Advancements in polymer chemistry have led to the synthesis of BCPs comprising conjugated rigid rod-coil,[51,52] rod-rod,[53–55] and pendent chromophore macromolecules,[56–59] resulting in a variety of photophysical properties driven by the electronic structure of the building blocks and block copolymer architecture. To the best of our knowledge, singlet fission dynamics in BCPs have not been reported to date. In order to characterize multiexciton dynamics in macromolecular systems, including exciton diffusion and transfer processes, we designed a BCP with an insulating

backbone of polynorbornene (PNo). The backbone serves as the scaffold furbished with a pendent pentacene derivative on one block and a tetracene derivative on the other block, **PePNo[m]-*b*-TePNo[n]** (where [m] and [n] are the number of repeat units of each block (Figure 1c). In this vein, we posit that altering the chemical composition of polymers with pendent chromophores, introducing a tetracene block with higher singlet and triplet energy levels than pentacene, can lead to a wealth of information about the complex potential energy surface and exciton diffusion. In fact, we find a complex energy conversion process in which both singlet and triplet exciton transfer occurs between the two blocks. Singlet resonant energy transfer is fast and efficient at short ranges, while triplet energy transfer is relatively inefficient and leads to considerable loss of triplet excitons generated far from the BCP interface. The fundamental multiexciton dynamics from this class of singlet fission block copolymers serve to bridge the gap of knowledge of exciton transport information between i(H)SF and x(H)SF chromophores – from individual molecules, to the mesoscale (BCPs, this study), and bulk crystalline systems.

Results and Discussion

In order to investigate how the composition of the iHSF BCPs affect multiexciton dynamics, a series of norbornene-based block copolymers with pendent pentacene and pendent tetracene units, **PePNo-*b*-TePNo**, were synthesized by ring-opening metathesis polymerization (Figure 1c, synthetic details in the section S5). In this study, we focus on maintaining a constant degree of polymerization of the block with the lower S_1 and T_1 energy states, **PePNo** (i.e. low-energy block; m = 10), while varying the length of the block with the higher energy states, **TePNo** (i.e. high-energy block; n = 5, 10, 20 and 40). Gel permeation chromatography (GPC) was used to confirm the molecular mass and to determine the dispersity of the polymer, Đ (See Table S9 in the SI for details). The steady-state absorption spectrum of **PePNo10-*b*-TePNo20** (Figure 2g) is a linear combination of the absorption spectrum of the two homopolymers, **PePNo10** and **TePNo20**, implying that no significant aggregation or charge transfer is occurring between the blocks in the ground state (see SI for additional details). The possible intramolecular singlet fission (iHSF) and energy transfer (ET) processes upon excitation of the tetracene block are shown in Figure 2. At short range, Dexter-type energy transfer processes dominate whereas FRET is more likely at long ranges (See SI page S4 for estimates). Here, we focus on exciting the high energy block to track

the exciton dynamics as the process moves "downhill" by singlet fission in the **TePNo** block, followed triplet transfer to the **PePNo** block (Figure 2, from $a \rightarrow b \rightarrow c \,/\, d \rightarrow f$); and/or by singlet energy transfer from **TePNo** to **PePNo**, subsequently undergoing SF to free triplets (Figure 2, from $a \rightarrow e \rightarrow d \rightarrow f$).

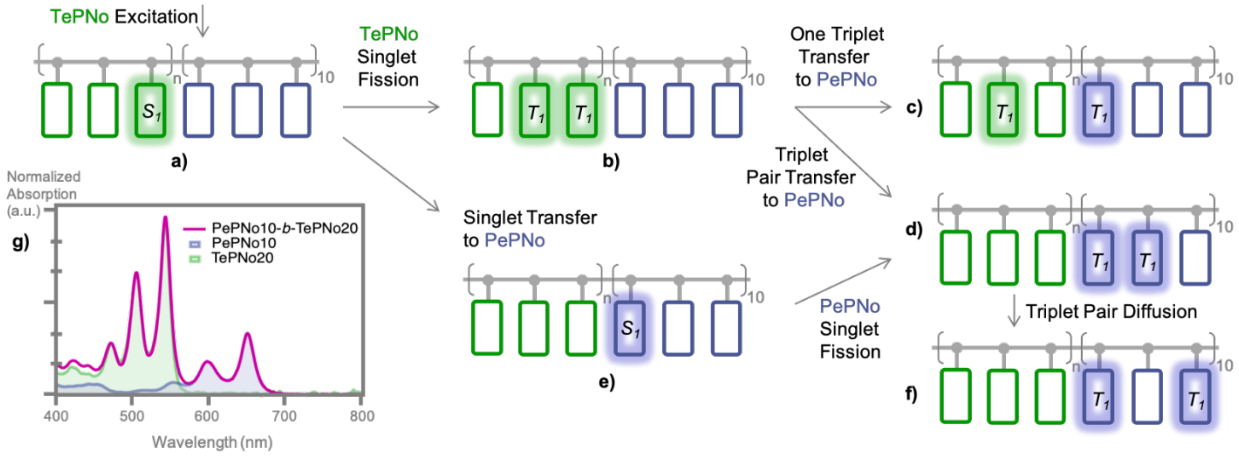

Figure 2. Possible exciton decay pathways in the block copolymer: Photoexcitation of the **TePNo** block produces a singlet exciton (**a**) that can decay via singlet fission into a triplet pair on the **TePNo** block (**b**), followed by triplet exciton transfer across the interface to the **PePNo** block (**c** and/or **d**). Alternatively, the singlet exciton on the **TePNo** block can undergo resonance energy transfer to produce a singlet exciton on the **PePNo** block (**e**), which can undergo SF to yield triplet pairs on the **PePNo** block (**d**, then **f**). **g**) Steady-state absorption spectrum of a block copolymer, **PePNo10-*b*-TePNo20** (pink trace), is shown for comparison to the two steady-state absorption spectra of the pentacene (purple) and tetracene (green) homopolymers, **PePNo10** and **TePNo20** respectively.

The BCP architecture provides a framework to study competing SF and charge/exciton transfer processes in a well-defined macromolecule having an interfacial energetic offset at the point of connectivity between two polymer blocks. The interface is well-defined, composed of one pentacene and one tetracene unit. To identify the key dynamical interfacial processes, we compare the exciton dynamics of the block copolymers to a pendent homopolymers of with either tetracene (**TePNo**) or pentacene repeat units. The pentacene control homopolymer (**PePNo**) and its iSF dynamics have been previously reported to demonstrate the efficacy of a new macromolecular

architectures with a known number of chromophores that exhibit SF.[36] Briefly, we summarize these previous results. By combining transient optical absorption with small angle-neutron scattering (SANS) and numerical modeling, we found that singlet fission occurs within an individual polymer chain that is free of aggregation, with a persistence length of ~ 5 repeat units. In polymer chains significantly longer than the persistence length, we observed a heterogeneous singlet fission process. Fast singlet decay was observed, arising from well-ordered or aligned chromophores along the chain, and slow singlet decay from aberrant pentacenes, as inferred by SANS data that shows that the homopolymer is compact and globule like (excluded volume parameter ~0.3). We found that the product of singlet fission was two free triplets that were mobile along the backbone of the polymer. A detailed analysis of the population dynamics showed that triplet pair annihilation proceeds though a secondary geminate process (triplets first diffuse apart then back together) following an Auger-like decay ($T_1 + T_1 \rightarrow T_1^* + S_0$) in which the product ($T_1^*$) is a hot triplet exciton.[60] The time scale for annihilation exhibits a linear dependence on the length until the saturation value is reached above ~ 20 repeat units.

In this study, we confirm that an isolated tetracene block is capable of generating triplet pairs via singlet fission by comparing the transient absorption data for tetracene norbornene monomer (**TeNo)** and a pendent tetracene homopolymer with twenty repeat units (**TePNo20**) (Figure 3a, b), which exhibit different population dynamics that reflect distinct triplet formation processes. The spectra associated with the singlets are nearly identical in both the monomer and polymer (Figure S4 and S5) and exhibit a transient signal with a ground-state bleach (GSB) feature at around 550 nm, stimulated emission (SE) at around 600 nm and broad photoinduced absorption (PIA) extending from 450 nm to 500 nm and 650 nm to 750 nm. In both **TeNo** and **TePNo20**, we observed an ultrafast (~8 ps) subtle shift of the singlet peak energies and amplitudes, consistent with a nuclear relaxation process (Figure S4 and S5). We note that minimal loss of population (change in the absolute magnitude of the GSB) or spin conversion (change in the ratio of the GSB to SE) is observed during this relaxation process. However, the transient spectra associated with the singlet species evolves much faster in **TePNo20** compared to **TeNo** (Figure 3a). In **TePNo20,** singlets primarily decay with a time constant of ~ 330 ps, a factor of three faster than in **TeNo** (Figure 3b). During this 330 ps time scale, the amplitude of the GSB stays nearly constant but the SE decays by more than 50%, indicative of a change in the excited state character rather than a loss of population (Figure S6). However, the observed singlet decay dynamics are heterogeneous

in **TePNo20**. A small singlet sub-ensemble is observed with a lifetime extending past several nanoseconds (Figure 3d), approaching the timescale of the **TeNo** singlet exciton (~ 11 ns). Overall, the singlet decay dynamics in **TePNo20** are characteristic of a singlet fission process. We note that the singlet exciton dynamics of the tetracene homopolymer is qualitatively similar to the pentacene homopolymer, showing a multiexponential (on average) SF process resulting from locally disordered pendent chromophores.

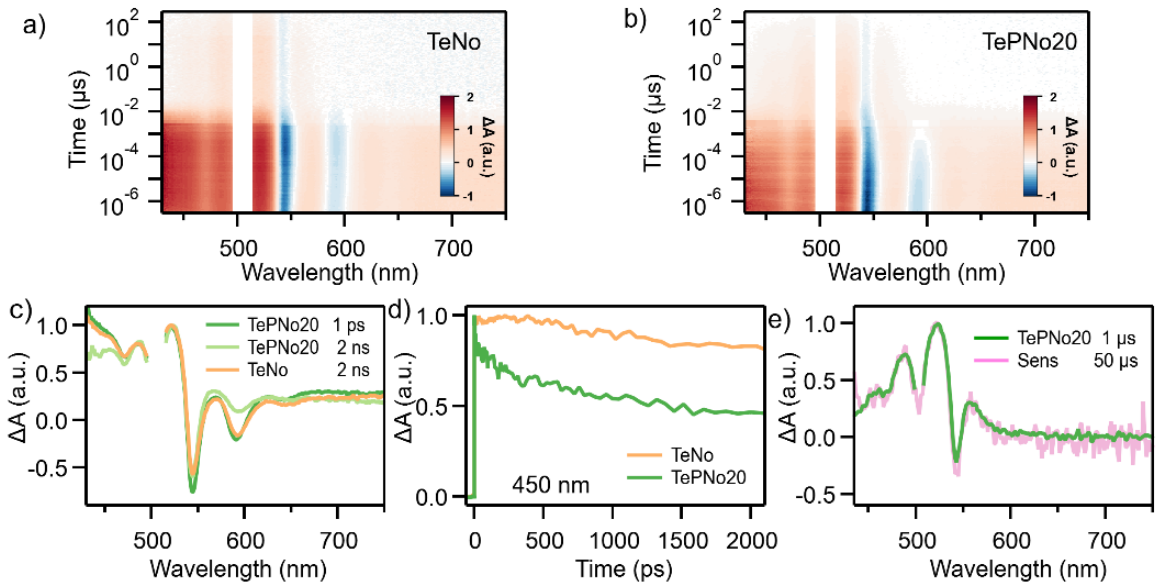

Figure 3. Singlet fission in tetracene monomer **TeNo** and homopolyer **TePNo20**. (**a**) Transient absorption spectrum of tetracene monomer **TeNo** in a dilute toluene solution excited at 505 nm (~50 μJ/cm^2) shows primarily singlet emission. A minority population of triplets is formed by intersystem crossing. (**b**) Transient absorption spectrum of **TePNo20** in toluene excited at 505 nm (~50 μJ/cm^2) shows that most singlets decay by singlet fission, resulting in a much greater population of triplets at long times (> 50 ns). (**c**) Spectral cut of **TePNo20** at early times (1 ps) are identical to the spectral cut of tetracene norbornene monomer singlet (**TeNo**, 2 ns), indicating that the singlet exciton is the same in both systems. The singlet signal of **TePNo20** (ESA ~ 450 nm and SE ~ 590 nm) decay faster from the spectral cut at 2 ns. (**d**) The singlet decay plots (~ 450 nm) of **TeNo** and **TePNo20** exhibit different decay channels. (**e**) Overlay of the triplet spectrum of the monomer generated by sensitization (pink line, Sens 50 μs) and the triplet spectrum obtained after singlet fission has occurred in the tetracene homopolymer (green line, **TePNo20** 1 μs).

The assignment of singlet fission is verified by comparison to triplet sensitization measurements, in which a triplet exciton is populated on the **TePNo20** polymer by collisional interactions with an anthracene donor. While the transient spectra associated with the long-lived product in **TePNo20** (green line, **TePNo20** 1 μs, Figure 3e) is identical to both the triplet sensitized polymer (pink line, Sens 50 μs, Figure 3e) and the long-lived species observed in the **TeNo** monomer (Figure 3c, S4 and S5), the decay kinetics of the **TePNo20** triplets indicate triplet pair character. In the **TeNo** monomer, triplets from intersystem crossing are generated on timescales of ~ 10 ns with a yield of ~ 20%, in agreement with what has been previously reported for TIPS-Tetracene.[24] For both triplet sensitization measurements and direct photoexcitation, the triplet population in **TeNo** monomer decays uniformly with a first order rate constant of ~ 100 μs. In contrast to **TeNo**, **TePNo20** exhibits the multiexponential decay dynamics associated with triplet pairs,[61,62] including the characteristic loss of ~ 50% of the amplitude on the ~ 1.5 μs time scale that results from an Auger-like annihilation mechanism [$^3(TT) \rightarrow S_0 + T_1$*, where T_1* is a hot triplet state].

An estimate of the triplet pair yield can be obtained by comparing the amplitude ratios of the stimulated emission features at different times (Figure 3b).[31] In **TePNo20**, we estimate the overall yield of triplet pairs generated in 330 ps conversion step is on the order of 35% (70% overall triplet yield, Figure S6). On longer timescales, a rigorous analysis becomes challenging due to experimental limitations that require changes of experimental geometries for delay times of > 6 ns, precluding quantitative comparison to the spectra at early time scales. However, as SF has been found to occur on 1- 10 nanosecond time scales in other related systems,[63] we can assume that some fraction of the remaining singlets will be converted to triplet pairs. To give a reasonable approximation for the upper limit of the total yield, we assume that 50% of the remaining singlets undergo SF yielding a ~ 135% total triplet yield, similar to what has been reported in tetracene crystals. This range of values is much less than what was observed in pendent pentacene polymers with similar structure, suggesting that the overall energetics of the system (slightly endothermic triplet pair formation) is a limiting factor for the overall yield.[24,37,38,62]

From these measurements and previous studies on **PePNo**, it is possible to extract important characteristics of the multiscale singlet exciton dynamics in these polymers driven by interfacial interactions. In highly ordered regions of the polymer, favorable chromophore overlap enables the formation of triplet pairs on a primary timescale of ~ 330 ps.[36,64] Singlet excitons formed in less ordered regions of the polymer persist for longer time scales, but can migrate to more favorable

sites via resonant energy transfer, or decay radiatively (into the far field). The end result is that singlet excitons are the primary species at early times (<100 ps), triplet pairs are the primary species from 10 – 1000 ns, and individual triplets are the primary species from 1 – 1000 μs. In the time window from ~ 100 ps to 10 ns, the co-existence of singlet and triplet excitons in the ensemble is observed. Similar dynamics have been observed in pendent pentacene polymers and flexible dimers.[36,64] Therefore, this phenomenon can be characterized as primarily resulting from disorder in the ensemble rather than dynamic interconversion in individual chains.

Having observed well-defined singlet fission characteristics of the **TePNo** and **PePNo** homopolymers, we turn to diblock copolymers (**PePNo[m]-*b*-TePNo[n]**) to study the dynamic exchange of excitons at their covalent interface. The marked spectral separation of the singlet transitions in tetracene and pentacene (Figure 2g) allows us to selectively excite either the pentacene or tetracene block. Furthermore, distinct spectroscopic signatures for triplets in pentacene and tetracene-based chromophores are well established and allow us to track the excited state population as a function of time. Therefore, these spectral signatures can be used to quantify the dynamics of singlet and triplet energy transfer, as the relative degree of polymerization (DP) of the tetracene and pentacene blocks are changed.

In a control experiment, direct excitation of the pentacene block leads to exciton dynamics that are nearly independent of the tetracene block length, suggesting minimal electronic perturbation. For example, resonant photoexcitation of the pentacene S_1 state (600 nm) in **PePNo10-*b*-TePNo[n]** BCP series resulted in transient signal features (as shown in Figure 4a-c and S9a) are similar to what is observed for the pendent pentacene homopolymer, **PePNo10** (Figure S7 and S8). At early times, the transient absorption spectrum signal is dominated by the photoinduced absorption feature at ~ 475 nm generated from the transition of the bright singlet state (S_1) to a higher energy singlet state (S_n). No spectral signature of direct photoexcitation of the tetracene blocks is observed, consistent with their near zero absorption at this wavelength. The singlet exciton rapidly evolves into a triplet exciton, which exhibits a photoinduced absorption feature at ~ 520 nm resulting from the transition from T_1 to T_n. Similar to what we have previously reported for the homopolymer, singlet fission occurs in high yield but shows inhomogeneity in the ensemble due to local disorder in the alignment of pendent chromophores.[36]

From the TA spectra and analysis as well as their similarity to the homopolymer system, the dynamics of the BCP are assigned to an excited state decay process of $S_1 \rightarrow (S_1 + TT) \rightarrow 2 \times T_1$.

Here, this notation is used to describe the dominant electronic configurations or mixture of configurations that are connected by the key kinetic transformations as a function of time. On average, the system can be characterized by set of rate constants in which subset of the singlets decay to triplet pairs in 50 ps and a second conversion step with a rate constant of ~ 1 ns. The $S_1 \rightarrow (S_1 + TT)$ dynamics show a very weak dependence on the overall BCP degree of polymerization, ranging from rate constants of 1.12 ns (**PePNo10-*b*-TePNo40**) to 1.43 ns (**PePNo10-*b*-TePNo5**). We note that these rates are slower on average than the comparable **PePNo** homopolymer (26 ps/800 ps). This suggests that the BCPs are slightly more disordered than the corresponding homopolymer, but that the degree of order increases with increasing DP of the tetracene block. Similar to the tetracene homopolymer described above, the triplet decay shows the characteristic triplet pair annihilation on time scales of 400-460 ns. Unlike the homopolymers, we note that the triplet lifetime shows a dependence on DP of the tetracene block, with recombination becoming faster as the degree of polymerization increases, ranging from 27 μs (**PePNo10-*b*-TePNo5**) to 8 μs (**PePNo10-*b*-TePNo40**). The decay kinetics are shown in the Figure S14. This result is unexpected given the known electronic structure of individual pentacene and tetracene chromophores, where charge or exciton transfer from pentacene to tetracene is energetically uphill. While the mechanism is currently unknown, we note that triplet-charge annihilation is spin allowed and has been shown to be fast in other systems.[65,66]

Photoexcitation of tetracene in the BCPs leads to exciton dynamics that are much different than the **TePNo** homopolymer and shows a strong dependence on the length of the tetracene block. This behavior is consistent with our expectation that both singlet and triplet energy transfer can occur and may be affected as the DP of the tetracene block changed. We note that under photoexcitation of the tetracene block, no dependence of the exciton dynamics on the pentacene DP is expected based on the electronic energy alignment between tetracene and pentacene (Figure 1). To minimize direct excitation of pentacene, we chose a pump pulse centered at 505 nm, which is resonant with the vibrationally excited S_1 state of tetracene and coincides with the transparent region between the S_1 and S_2 pentacene excitons (Figure 2g). At the early times, the transient absorption spectra are dominated by tetracene singlets showing identical spectral characteristics to **TePNo[n],** including a photoinduced absorption signal from 430 - 540 nm and 650 – 750 nm, ground state bleaching at 545 nm, and stimulated emission at 600 nm (as shown in Figure 4d-f and S9b). There is no measurable direct excitation of pentacene singlets, which would result in an

instantaneous ground state bleach feature at 660 nm. With increasing time delay (100-200 ps), the signals of the pentacene ground state bleach emerge as the tetracene signals decay. We note that unlike other small molecule and blended thin film systems, no direct iHSF process is observed since 1) direct absorption at the tetracene-pentacene interface is statistically unlikely and 2) the interfacial triplet pair is higher in energy than the bulk triplet pair.[6]

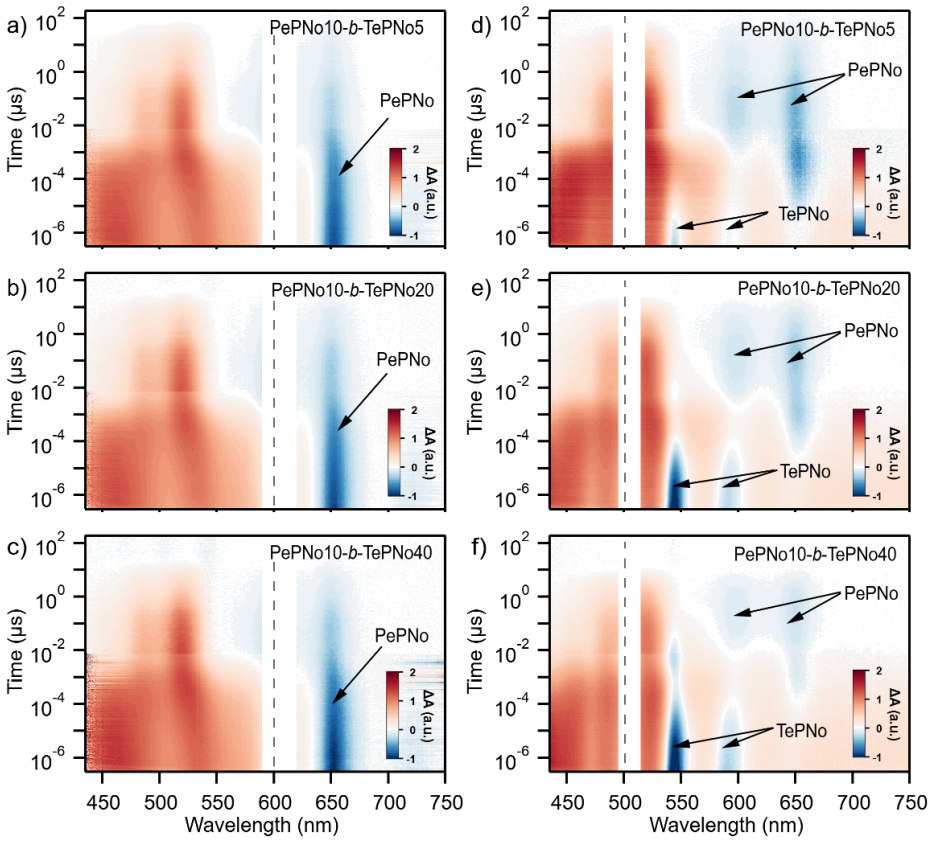

Figure 4. Transient absorption spectroscopy of **PePNo10-*b*-TePNo[n]** block copolymers in toluene solution at dilute concentrations (< 100 μM). The pump wavelength is 600 nm (**PePNo** block excitation; **a**, **b**, **c**) and 505 nm (**TePNo** block excitation; **d**, **e**, **f**).

As **TePNo** excitons exhibit a photoinduced absorption feature and **PePNo** excitons exhibit a negative ground state bleaching signal, their relative concentration as a function of time determines net sign of the measured signals near 660 nm (Figure 4d-f). The relative concentration is influenced by both the instantaneous number of excitons generated by the laser pulse and the rate of exciton conversion from **TePNo** to **PePNo**. The early time dynamics indicate a larger population of **TePNo** singlet excitons for longer block lengths. This causes the net signal to switch sign from positive to

negative at later times (2 ps → 9 ps → 30 ps → 140 ps), even though the measured rate constants describing the emergence of the pentacene bleach (Figure S15) are nearly the same (20 ps and 200 ps) in all but **PePNo10-b-TePNo5** (10 and 110 ps). Using time-correlated single photon counting methods (Figure S3), we measured the emission dynamics at 565 nm (tetracene singlet) and 675 nm (pentacene singlet). An obvious rise near the pentacene peak with a time constant of ~200 ps shows that fast singlet energy transfer occurs from high energy tetracene singlet to pentacene. This time constant is consistent with the fast rise of the pentacene signal observed in the transient absorption spectra, suggesting that singlet exciton transfer is a major contributing decay pathway. The tetracene emission is not coincident with the rise of pentacene emission decay. The tetracene signal decays biexponentially (~500 ps and 2 ns), similar to what is observed in the **TePNo20** homopolymer. As such, we conclude that the tetracene PL signal is dominated by persistent singlets generated far from the BCP covalent interface. Taken together, the data infers that the rapid quenching of tetracene singlets via resonance energy transfer is dominated by excitations generated near the **TePNo**/**PePNo** interface. However, for excitations generated far from the interface, energy transfer is too slow to compete with singlet fission on the tetracene block, resulting in a larger fraction of persistent **TePNo** excitons as the block length increases.

In addition to singlet exciton transfer at early times, we observed an additional, slower triplet exciton transfer process with a relative dependence on the **TePNo** DP. This effect can be clearly seen by comparing the transient spectra at a selected time delay from several nanoseconds to microseconds (Figure 5a, d; and Figure S20a, d). For **PePNo10-*b*-TePNo5**, the superimposed GSB signal from tetracene (~ 540 nm) is unresolvable by 5 ns and only the GSB signal of pentacene is apparent. As such, energy transfer from tetracene to pentacene is complete by this time, with the primary contribution coming from fast singlet energy transfer. In contrast, for **PePNo10-*b*-TePNo40**, the GSB of tetracene is still apparent at 100 ns, and its disappearance is accompanied by an increase in the relative amplitude of the pentacene GSB signal near 660 nm. After several microseconds, the spectra indicate that only triplet exciton on the **PePNo** block remains. Analyzing kinetic traces at 460 nm (the blue edge of triplet ESA), 544 nm (superposition of red side of triplet ESA and tetracene GSB), and 650 nm (pentacene GSB), the interconversion dynamics between the different species were monitored. In **PePNo10-*b*-TePNo5** (Figure 5b), we observe a net positive signal at 544 nm and the same decay dynamics for all three probe wavelengths, confirming that energy transfer to the **PePNo** block was complete in less than 5 ns. In contrast, **PePNo10-*b*-**

TePNo40 (Figure 5e) shows an obvious net negative signal near 544 nm at early times, indicating the existence of a tetracene triplet population. The tetracene triplet signals decays (becoming net positive at 544 nm) over hundreds of nanoseconds as additional pentacene triplets form (increasing the amplitude of the GSB signals at 650 nm). We conclude that triplet energy transfer is occurring since a sub-ensemble of tetracene triplet excitons show decay coincident with the slow rise of the pentacene GSB signal in **PePNo10-*b*-TePNo40**. In addition, we find a sub-ensemble of tetracene triplets that decay on time scales that do not match the pentacene GSB dynamics. This indicates that these triplets are trapped on the **TePNo40** block and recombine before reaching the interface.

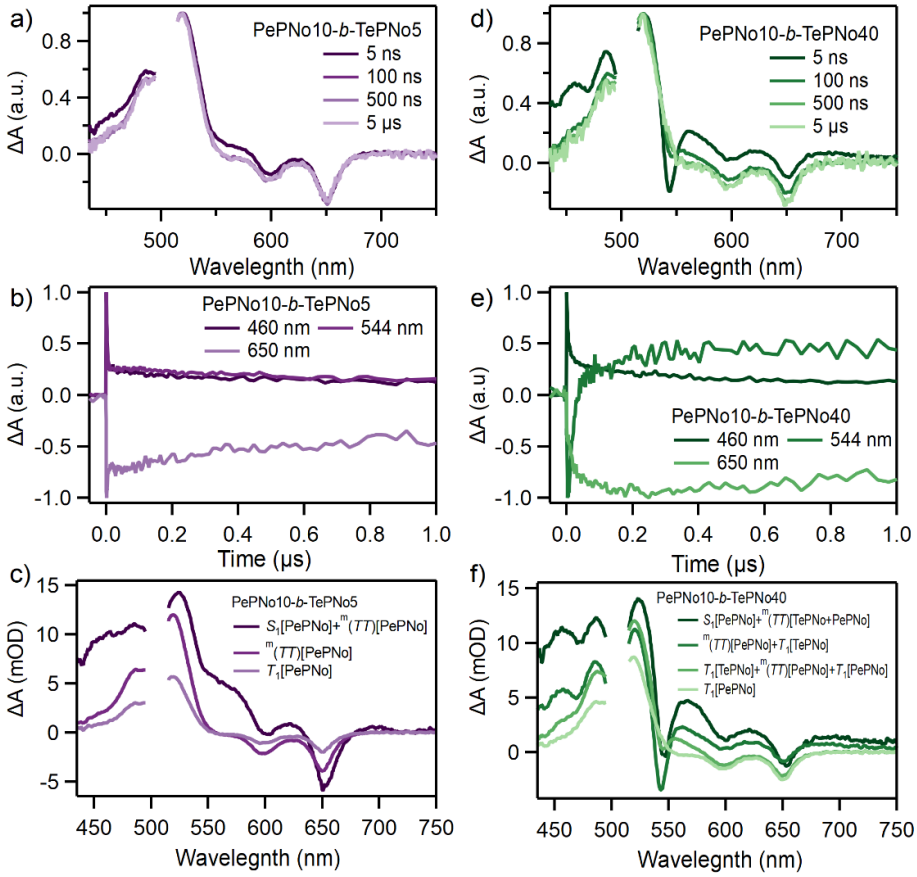

Figure 5. Transient spectra at selected delay times along with kinetic traces at probe wavelengths of 460, 544 and 650 nm of ns-TA data from **PePNo10-b-TePNo5** (**a**,**b**) and **PePNo10-b-TePNo40** (**d**,**e**). **c**) Global analysis of ns-TA data of **PePNo10-*b*-TePNo5**, where the signals are assigned as follows: species 1: S_1[PePNo-block] + $^{m}(TT)$[PePNo-block]; species 2: $^{m}(TT)$[PePNo-block]; species 3: T_1[PePNo-block]. **f**) Global analysis of ns-TA data of **PePNo10-*b*-TePNo40**, where the signals are assigned as follows: species 1: S_1[PePNo-block] + $^{m}(TT)$[PePNo and TePNo blocks];

species 2: $^{m}(TT)$[PePNo-block] + T_1[TePNo-block]; species 3: T_1[PePNo-block] + T_1[TePNo-block] + $^{m}(TT)$[PePNo-block]; species 4: T_1[PePNo-block].

The data, in aggregate, allows us to construct a comprehensive model for the exciton dynamics of the BCPs as a function of DP. To buttress the data interpretation, we performed a global analysis of the fs- (Figure S16-19) and ns-TA data (Figure 5c, f and Figure S20c, f) using a sequential decay model. The model isolates the transient spectra corresponding to each species, which can consist of a mixture of different electronic configurations, that exhibits a characteristic decay rate. These species are assigned based on their comparison to the spectra and decay kinetics in the homopolymer and by comparison to supporting measurements (e.g., TRPL and triplet sensitization). We will discuss only the short and long limiting cases here, but a summary of the overall dynamics for all block lengths can be found in Table 1 and in Section 3 of the SI. In the BCP with the shortest tetracene block, **PePNo10-*b*-TePNo5**, singlet excitons generated on **TePNo** decay primarily by resonant energy transfer to **PePNo** on time scales (< 100 ps) that outcompete singlet fission of tetracene (~ 300 ps). This corresponds to path $a \rightarrow e \rightarrow d \rightarrow f$ in Figure 2, where the excited state population is nearly entirely transferred from **TePNo5** to **PePNo10** on ultrafast time scales. The subsequent dynamics of the block copolymer resemble the **PePNo** homopolymer: singlet fission in **PePNo10** to generate $^{m}(TT)$ over multiple time scales (ensemble average). Subsequently triplet-triplet annihilation follows a secondary geminate process in which triplet pairs separate then recombine. The signature of the secondary geminate process is the rapid loss of 50% of the excited state population (~ 500 ns), followed by a decay of the remaining population (T_1) at the individual triplet lifetime, as determined by sensitization experiments (~ 23 μs).

In the BCP with the longest tetracene block, **PePNo10-*b*-TePNo40**, the dynamics are much more complex. Tetracene singlet excitons generated near the tetracene-pentacene interface are still efficiently transferred to the pentacene block by resonant energy transfer. However, a sub-ensemble of excitons are generated on chromophores further from the interface, such that singlet fission now kinetically outcompetes resonant energy transfer. The result is an instantaneous population of tetracene triplet pairs and pentacene singlets: $^{m}(TT)$[**TePNo**] + S_1[**PePNo**] (paths $a \rightarrow b$ and path $a \rightarrow e$ in Figure 2). Subsequent singlet fission on the **PePNo** block results in a heterogenous evolution to a state where tetracene triplet pairs, pentacene singlets, and pentacene triplet pairs all coexist in the ensemble ($^{m}(TT)$[**TePNo**] + S_1[**PePNo**] + $^{m}(TT)$[**PePNo**]) until SF is

complete (paths $b \rightarrow c, d$ and path $e \rightarrow d$ in Figure 2). We then observe an ensemble average in which both tetracene and pentacene triplet pairs are populated: $^{m}(TT)$[**TePNo**] + $^{m}(TT)$[**PePNo**] (Figures 2b, 2d, and 5f). It is important to note that under these excitation conditions, there is a vanishingly small probability of exciting any individual polymer chain more than once. Therefore, the resulting triplet decay dynamics that we observe are a mix of BCPs with tetracene triplet pairs (SF in **TePNo** faster than FRET) and pentacene triplet pairs (FRET faster than SF in **TePNo**). For individual BCPs with pentacene triplet pairs, the decay dynamics are analogous to the **PePNo10-*b*-TePNo5** or the homopolymer, where secondary geminate recombination dominates on the a few hundred nanosecond time scale. However, triplets generated on the **TePNo** block can undergo triplet-triplet annihilation or diffuse and undergo triplet energy transfer to the pentacene block, resulting in one triplet on **TePNo** and one on **PePNo**. The net result is a mixture of tetracene triplets, pentacene triplets, and triplet pairs: T_1[**TePNo**] + $^{m}(TT)$[**PePNo**] + T_1[**PePNo**] (Figure 5f and 2c, 2d, 2f). As discussed above, the lifetime of an individual triplet on pentacene T_1[**PePNo**] is much longer than the triplet pair $^{m}(TT)$[**PePNo**]. This allows us to use kinetic considerations for both their formation and decay to distinguish triplets on **PePNo** populated by SF and those populated by triplet energy transfer. Interestingly, we find that the final species consists of solely pentacene triplets T_1[**PePNo**] (Figure 5f, and 2f) despite the longer intrinsic lifetime of T_1[**TePNo**], suggesting that downhill energy transfer of triplets is an efficient process. A similar observation has been made in covalently bound tetracene-pentacene dimers.[26]

The time-resolved optical data sets allow us to quantify the overall probability of transferring an exciton created on the **TePNo** block to the **PePNo** block, as well as the method of transfer (singlet *versus* triplet energy transfer). The overall internal exciton transfer probability is defined as $\Phi_{IET} = (n_{SET} + n_{TET})/(n_{SET} + n_{TET} + n_D)$, where n_{SET} (n_{TET}) is the number of excitons that undergo singlet (triplet) energy transfer and n_D is the number of excitons that decay directly on the **TePNo** block. This metric can be considered analogous to an internal quantum yield in other operational systems, as it is an estimate of the "harvesting" efficiency per photon absorbed. The probability that an exciton directly decays on the tetracene block is then $(1 - \Phi_{IET})$. The procedure for determining Φ_{IET} and the relative fractions of excitons transferred via singlet ($n_{SET}/(n_{SET} + n_{TET})$) or triplet ($n_{TET}/(n_{SET} + n_{TET})$) energy transfer can be calculated using reasonable assumptions that are described in detail in the Supporting Information. In brief, for each "species" derived from global analysis, we quantify the total instantaneous population of excitons

and their distribution between **TePNo** to **PePNo** using their respective ground state bleach intensities (Figure S21). Following this analysis, we determine the relative contributions of triplets populated via iSF versus those populated from triplet energy transfer by considering kinetic arguments governing their formation and decay. For example, an increase in the pentacene GSB at time scales much longer than the singlet exciton lifetime can only result from triplet energy transfer, as described above. A similar analysis using the excited state absorption signals rather than the GSB verifies this procedure and allows us to further identify a fraction of "trapped" tetracene triplet excitons that decay directly on the tetracene block. A summary of the relative yields of singlet versus triplet energy transfer and overall Φ_{IET} are shown in Table 1.

Table 1. Internal exciton transfer yield (Φ_{IET}) and the relative fractions of singlet (SET) and triplet exciton transfer (TET) for the polymers with varying degrees of polymerization.

Diblock polymers	Φ_{IET}	SET Fraction	TET Fraction
PePNo10-*b*-TePNo5	1	1	0
PePNo10-*b*-TePNo10	0.5	0.85	0.15
PePNo10-*b*-TePNo20	0.4	0.71	0.29
PePNo10-*b*-TePNo40	0.2	0.46	0.54

Conclusion

In this study, diblock copolymers were designed to develop structure-property relationships of multiexciton processes. These systems reveal a wealth of quantifiable information about energy transfer and transport processes within macromolecules, as we develop a fundamental connection between small molecule and bulk solid-state multiexciton dynamics. The studies here imply that tetracene-based systems that are driven by singlet fission are likely to be inefficient for triplet exciton diffusion. For example, though the fraction of triplet transfer to the overall PePNo population increases as a function of length, from 0 in **TePNo5** to > 50% in **TePNo40**, the overall Φ_{IET} for exciton transfer drops precipitously, from 1 to 0.2. We observe heterogeneous triplet energy transfer rates in the ensemble, ranging from 10s to 100s of nanoseconds, with the dominant energy transfer process in **TePNo40** occurring in ~ 250 ns. This suggests a large fraction of trapped triplet excitons for all but the shortest **TePNo** block, since these time scales on the whole are still much significantly shorter than the triplet lifetime. We note that transient microscopy studies

reached a similar conclusion – contributions from singlet energy transfer greatly enhance the spatial movement of excitons in tetracene.[17] Our data here adds a perspective to this problem: since triplet diffusivity in tetracene is likely to be low for a subset of non-localized triplet excitons, the presence of disorder in the system means that the vast majority of triplet excitons are localized and immobile. As a result, previous estimates for tetracene, though already low, may in fact represent an overestimate of average diffusivity of the full ensemble. Interestingly, the singlet fission dynamics of the **PePNo** homopolymer and thin-films of pentacene-based tetramers[34,36,67] suggest that triplet diffusivity is reasonably efficient and that localization of triplets from disorder is not necessarily a universal phenomenon for all SF materials. Further studies are underway to quantify the triplet exciton transfer probability between individual chromophores, and developing models to understand multiexciton dynamics in the mesoscale.

Supporting Information

The Supporting Information is available free of charge on the ACS Publications website. Supporting Information includes experimental details, such as synthetic methods and characterization, spectroscopic data and analysis, Supplementary Figures, and Supplementary Tables.

Acknowledgment

This work was supported by the National Science Foundation under grants DMR-2004683 and DMR-2004678. K.R.P. thanks the Department of Defense for a National Defense Science and Engineering (NDSEG) Fellowship. This research used resources at the Center for Functional Nanomaterials, which is a U.S. DOE Office of Science Facility at Brookhaven National Laboratory under contract DE-SC0012704. We thank Dr. Samuel Sanders, Dr. Elango Kumarasamy, and Dr. Hua Li for insightful discussions.

Graphical Table of Contents

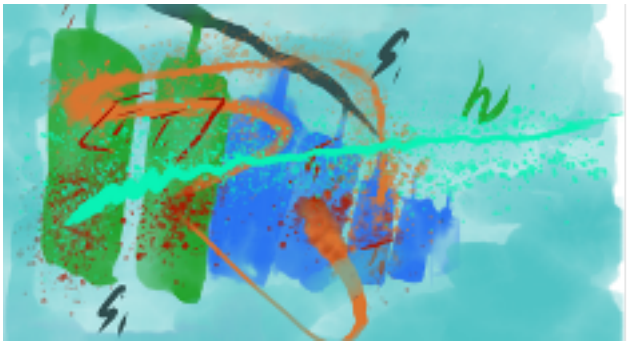

References

(1) Lee, J.; Jadhav, P.; Reusswig, P. D.; Yost, S. R.; Thompson, N. J.; Congreve, D. N.; Hontz, E.; Van Voorhis, T.; Baldo, M. A. Singlet Exciton Fission Photovoltaics. *Acc. Chem. Res.* **2013**, *46* (6), 1300–1311. https://doi.org/10.1021/ar300288e.

(2) Xia, J.; Sanders, S. N.; Cheng, W.; Low, J. Z.; Liu, J.; Campos, L. M.; Sun, T. Singlet Fission: Progress and Prospects in Solar Cells. *Adv. Mater.* **2017**, *29* (20), 1601652. https://doi.org/10.1002/adma.201601652.

(3) Lee, J.; Jadhav, P.; Baldo, M. A. High Efficiency Organic Multilayer Photodetectors Based on Singlet Exciton Fission. *Appl. Phys. Lett.* **2009**, *95* (3), 033301. https://doi.org/10.1063/1.3182787.

(4) Schrauben, J. N.; Zhao, Y.; Mercado, C.; Dron, P. I.; Ryerson, J. L.; Michl, J.; Zhu, K.; Johnson, J. C. Photocurrent Enhanced by Singlet Fission in a Dye-Sensitized Solar Cell. *ACS Appl. Mater. Interfaces* **2015**, *7* (4), 2286–2293. https://doi.org/10.1021/am506329v.

(5) Shockley, W.; Queisser, H. J. Detailed Balance Limit of Efficiency of P-n Junction Solar Cells. *J. Appl. Phys.* **1961**, *32* (3), 510–519. https://doi.org/10.1063/1.1736034.

(6) Pun, A. B.; Asadpoordarvish, A.; Kumarasamy, E.; Tayebjee, M. J. Y.; Niesner, D.; McCamey, D. R.; Sanders, S. N.; Campos, L. M.; Sfeir, M. Y. Ultra-Fast Intramolecular Singlet Fission to Persistent Multiexcitons by Molecular Design. *Nat. Chem.* **2019**, *11* (9), 821–828. https://doi.org/10.1038/s41557-019-0297-7.

(7) Sanders, S. N.; Pun, A. B.; Parenti, K. R.; Kumarasamy, E.; Yablon, L. M.; Sfeir, M. Y.; Campos, L. M. Understanding the Bound Triplet-Pair State in Singlet Fission. *Chem* **2019**, *5* (8), 1988–2005. https://doi.org/10.1016/j.chempr.2019.05.012.

(8) Wang, Z.; Liu, H.; Xie, X.; Zhang, C.; Wang, R.; Chen, L.; Xu, Y.; Ma, H.; Fang, W.; Yao, Y.; Sang, H.; Wang, X.; Li, X.; Xiao, M. Free-Triplet Generation with Improved Efficiency in Tetracene Oligomers through Spatially Separated Triplet Pair States. *Nat. Chem.* **2021**, *13* (6), 559–567. https://doi.org/10.1038/s41557-021-00665-7.

(9) Han, S.; Deng, R.; Gu, Q.; Ni, L.; Huynh, U.; Zhang, J.; Yi, Z.; Zhao, B.; Tamura, H.; Pershin, A.; Xu, H.; Huang, Z.; Ahmad, S.; Abdi-Jalebi, M.; Sadhanala, A.; Tang, M. L.; Bakulin, A.; Beljonne, D.; Liu, X.; Rao, A. Lanthanide-Doped Inorganic Nanoparticles Turn Molecular Triplet Excitons Bright. *Nature* **2020**, *587* (7835), 594–599. https://doi.org/10.1038/s41586-020-2932-2.

(10) Rao, A.; Friend, R. H. Harnessing Singlet Exciton Fission to Break the Shockley–Queisser Limit. *Nat. Rev. Mater.* **2017**, *2* (11), 17063. https://doi.org/10.1038/natrevmats.2017.63.

(11) Einzinger, M.; Wu, T.; Kompalla, J. F.; Smith, H. L.; Perkinson, C. F.; Nienhaus, L.; Wieghold, S.; Congreve, D. N.; Kahn, A.; Bawendi, M. G.; Baldo, M. A. Sensitization of Silicon by Singlet Exciton Fission in Tetracene. *Nature* **2019**, *571* (7763), 90–94. https://doi.org/10.1038/s41586-019-1339-4.
(12) Ehrler, B.; Musselman, K. P.; Böhm, M. L.; Friend, R. H.; Greenham, N. C. Hybrid Pentacene/a-Silicon Solar Cells Utilizing Multiple Carrier Generation via Singlet Exciton Fission. *Appl. Phys. Lett.* **2012**, *101* (15), 153507. https://doi.org/10.1063/1.4757612.
(13) Yang, L.; Tabachnyk, M.; Bayliss, S. L.; Böhm, M. L.; Broch, K.; Greenham, N. C.; Friend, R. H.; Ehrler, B. Solution-Processable Singlet Fission Photovoltaic Devices. *Nano Lett.* **2015**, *15* (1), 354–358. https://doi.org/10.1021/nl503650a.
(14) MacQueen, R. W.; Liebhaber, M.; Niederhausen, J.; Mews, M.; Gersmann, C.; Jäckle, S.; Jäger, K.; Tayebjee, M. J. Y.; Schmidt, T. W.; Rech, B.; Lips, K. Crystalline Silicon Solar Cells with Tetracene Interlayers: The Path to Silicon-Singlet Fission Heterojunction Devices. *Mater. Horiz.* **2018**, *5* (6), 1065–1075. https://doi.org/10.1039/C8MH00853A.
(15) Kozlov, O. V.; de Haan, F.; Kerner, R. A.; Rand, B. P.; Cheyns, D.; Pshenichnikov, M. S. Real-Time Tracking of Singlet Exciton Diffusion in Organic Semiconductors. *Phys. Rev. Lett.* **2016**, *116* (5), 057402. https://doi.org/10.1103/PhysRevLett.116.057402.
(16) Wan, Y.; Guo, Z.; Zhu, T.; Yan, S.; Johnson, J.; Huang, L. Cooperative Singlet and Triplet Exciton Transport in Tetracene Crystals Visualized by Ultrafast Microscopy. *Nat. Chem.* **2015**, *7* (10), 785–792. https://doi.org/10.1038/nchem.2348.
(17) Zhu, T.; Wan, Y.; Guo, Z.; Johnson, J.; Huang, L. Two Birds with One Stone: Tailoring Singlet Fission for Both Triplet Yield and Exciton Diffusion Length. *Adv. Mater.* **2016**, *28* (34), 7539–7547. https://doi.org/10.1002/adma.201600968.
(18) Carlotti, B.; Madu, I. K.; Kim, H.; Cai, Zhengxu.; Jiang, H.; Muthike, A. K.; Yu, L.; Zimmerman, P. M.; Goodson, T. Activating Intramolecular Singlet Exciton Fission by Altering π-Bridge Flexibility in Perylene Diimide Trimers for Organic Solar Cells. *Chem. Sci.* **2020**, *11* (33), 8757–8770. https://doi.org/10.1039/D0SC03271A.
(19) Low, J. Z.; Sanders, S. N.; Campos, L. M. Correlating Structure and Function in Organic Electronics: From Single Molecule Transport to Singlet Fission. *Chem. Mater.* **2015**, *27* (16), 5453–5463. https://doi.org/10.1021/cm502366x.
(20) Young, R. M.; Wasielewski, M. R. Mixed Electronic States in Molecular Dimers: Connecting Singlet Fission, Excimer Formation, and Symmetry-Breaking Charge Transfer. *Acc. Chem. Res.* **2020**, *53* (9), 1957–1968. https://doi.org/10.1021/acs.accounts.0c00397.
(21) Ullrich, T.; Munz, D.; Guldi, D. M. Unconventional Singlet Fission Materials. *Chem. Soc. Rev.* **2021**, *50* (5), 3485–3518. https://doi.org/10.1039/D0CS01433H.
(22) Tilley, A. J.; Pensack, R. D.; Kynaston, E. L.; Scholes, G. D.; Seferos, D. S. Singlet Fission in Core–Shell Micelles of End-Functionalized Polymers. *Chem. Mater.* **2018**, *30* (13), 4409–4421. https://doi.org/10.1021/acs.chemmater.8b01814.
(23) Walker, B. J.; Musser, A. J.; Beljonne, D.; Friend, R. H. Singlet Exciton Fission in Solution. *Nat. Chem.* **2013**, *5*, 1019. https://doi.org/10.1038/nchem.1801.
(24) Stern, H. L.; Musser, A. J.; Gelinas, S.; Parkinson, P.; Herz, L. M.; Bruzek, M. J.; Anthony, J.; Friend, R. H.; Walker, B. J. Identification of a Triplet Pair Intermediate in Singlet Exciton Fission in Solution. *Proc. Natl. Acad. Sci.* **2015**, *112* (25), 7656–7661. https://doi.org/10.1073/pnas.1503471112.

(25) Sanders, S. N.; Kumarasamy, E.; Pun, A. B.; Steigerwald, M. L.; Sfeir, M. Y.; Campos, L. M. Intramolecular Singlet Fission in Oligoacene Heterodimers. *Angew. Chem. Int. Ed.* **2016**, *55* (10), 3373–3377. https://doi.org/10.1002/anie.201510632.
(26) Sanders, S. N.; Kumarasamy, E.; Pun, A. B.; Appavoo, K.; Steigerwald, M. L.; Campos, L. M.; Sfeir, M. Y. Exciton Correlations in Intramolecular Singlet Fission. *J. Am. Chem. Soc.* **2016**, *138* (23), 7289–7297. https://doi.org/10.1021/jacs.6b00657.
(27) Zeiser, C.; Moretti, L.; Lepple, D.; Cerullo, G.; Maiuri, M.; Broch, K. Singlet Heterofission in Tetracene–Pentacene Thin-Film Blends. *Angew. Chem. Int. Ed.* **2020**, *59* (45), 19966–19973. https://doi.org/10.1002/anie.202007412.
(28) Wan, Y.; Wiederrecht, G. P.; Schaller, R. D.; Johnson, J. C.; Huang, L. Transport of Spin-Entangled Triplet Excitons Generated by Singlet Fission. *J. Phys. Chem. Lett.* **2018**, *9* (23), 6731–6738. https://doi.org/10.1021/acs.jpclett.8b02944.
(29) Folie, B. D.; Haber, J. B.; Refaely-Abramson, S.; Neaton, J. B.; Ginsberg, N. S. Long-Lived Correlated Triplet Pairs in a π-Stacked Crystalline Pentacene Derivative. *J. Am. Chem. Soc.* **2018**, *140* (6), 2326–2335. https://doi.org/10.1021/jacs.7b12662.
(30) Munson, K. T.; Gan, J.; Grieco, C.; Doucette, G. S.; Anthony, J. E.; Asbury, J. B. Ultrafast Triplet Pair Separation and Triplet Trapping Following Singlet Fission in Amorphous Pentacene Films. *J. Phys. Chem. C* **2020**, *124* (43), 23567–23578. https://doi.org/10.1021/acs.jpcc.0c07920.
(31) Sanders, S. N.; Kumarasamy, E.; Pun, A. B.; Trinh, M. T.; Choi, B.; Xia, J.; Taffet, E. J.; Low, J. Z.; Miller, J. R.; Roy, X.; Zhu, X. Y.; Steigerwald, M. L.; Sfeir, M. Y.; Campos, L. M. Quantitative Intramolecular Singlet Fission in Bipentacenes. *J. Am. Chem. Soc.* **2015**, *137* (28), 8965–8972. https://doi.org/10.1021/jacs.5b04986.
(32) Sanders, S. N.; Kumarasamy, E.; Pun, A. B.; Steigerwald, M. L.; Sfeir, M. Y.; Campos, L. M. Intramolecular Singlet Fission in Oligoacene Heterodimers. *Angew. Chem. Int. Ed.* **2016**, *55* (10), 3373–3377. https://doi.org/10.1002/anie.201510632.
(33) Sanders, S. N.; Kumarasamy, E.; Fallon, K. J.; Sfeir, M. Y.; Campos, L. M. Singlet Fission in a Hexacene Dimer: Energetics Dictate Dynamics. *Chem. Sci.* **2020**, *11* (4), 1079–1084. https://doi.org/10.1039/C9SC05066C.
(34) Huang, H.; He, G.; Xu, K.; Wu, Q.; Wu, D.; Sfeir, M. Y.; Xia, J. Achieving Long-Lived Triplet States in Intramolecular SF Films through Molecular Engineering. *Chem* **2019**, *5* (9), 2405–2417. https://doi.org/10.1016/j.chempr.2019.06.007.
(35) Sanders, S. N.; Kumarasamy, E.; Pun, A. B.; Steigerwald, M. L.; Sfeir, M. Y.; Campos, L. M. Singlet Fission in Polypentacene. *Chem* **2016**, *1* (3), 505–511. https://doi.org/10.1016/j.chempr.2016.08.016.
(36) Yablon, L. M.; Sanders, S. N.; Li, H.; Parenti, K. R.; Kumarasamy, E.; Fallon, K. J.; Hore, M. J. A.; Cacciuto, A.; Sfeir, M. Y.; Campos, L. M. Persistent Multiexcitons from Polymers with Pendent Pentacenes. *J. Am. Chem. Soc.* **2019**, *141* (24), 9564–9569. https://doi.org/10.1021/jacs.9b02241.
(37) Korovina, N. V.; Joy, J.; Feng, X.; Feltenberger, C.; Krylov, A. I.; Bradforth, S. E.; Thompson, M. E. Linker-Dependent Singlet Fission in Tetracene Dimers. *J. Am. Chem. Soc.* **2018**, *140* (32), 10179–10190. https://doi.org/10.1021/jacs.8b04401.
(38) Pun, A. B.; Sanders, S. N.; Kumarasamy, E.; Sfeir, M. Y.; Congreve, D. N.; Campos, L. M. Triplet Harvesting from Intramolecular Singlet Fission in Polytetracene. *Adv. Mater.* **2017**, *29* (41), 1701416. https://doi.org/10.1002/adma.201701416.

(39) Busby, E.; Xia, J.; Wu, Q.; Low, J. Z.; Song, R.; Miller, J. R.; Zhu, X.-Y.; Campos, L. M.; Sfeir, M. Y. A Design Strategy for Intramolecular Singlet Fission Mediated by Charge-Transfer States in Donor–Acceptor Organic Materials. *Nat. Mater.* **2015**, *14* (4), 426–433. https://doi.org/10.1038/nmat4175.
(40) Wang, L.; Liu, X.; Shi, X.; Anderson, C. L.; Klivansky, L. M.; Liu, Y.; Wu, Y.; Chen, J.; Yao, J.; Fu, H. Singlet Fission in a *Para* -Azaquinodimethane-Based Quinoidal Conjugated Polymer. *J. Am. Chem. Soc.* **2020**, *142* (42), 17892–17896. https://doi.org/10.1021/jacs.0c06604.
(41) Hu, J.; Xu, K.; Shen, L.; Wu, Q.; He, G.; Wang, J.-Y.; Pei, J.; Xia, J.; Sfeir, M. Y. New Insights into the Design of Conjugated Polymers for Intramolecular Singlet Fission. *Nat. Commun.* **2018**, *9* (1), 2999. https://doi.org/10.1038/s41467-018-05389-w.
(42) He, G.; Busby, E.; Appavoo, K.; Wu, Q.; Xia, J.; Campos, L. M.; Sfeir, M. Y. Charge Transfer States Impact the Triplet Pair Dynamics of Singlet Fission Polymers. *J. Chem. Phys.* **2020**, *153* (24), 244902. https://doi.org/10.1063/5.0029858.
(43) Kasai, Y.; Tamai, Y.; Ohkita, H.; Benten, H.; Ito, S. Ultrafast Singlet Fission in a Push–Pull Low-Bandgap Polymer Film. *J. Am. Chem. Soc.* **2015**, *137* (51), 15980–15983. https://doi.org/10.1021/jacs.5b09361.
(44) Liu, X.; He, B.; Garzón-Ruiz, A.; Navarro, A.; Chen, T. L.; Kolaczkowski, M. A.; Feng, S.; Zhang, L.; Anderson, C. A.; Chen, J.; Liu, Y. Unraveling the Main Chain and Side Chain Effects on Thin Film Morphology and Charge Transport in Quinoidal Conjugated Polymers. *Adv. Funct. Mater.* **2018**, *28* (31), 1801874. https://doi.org/10.1002/adfm.201801874.
(45) Pace, N. A.; Zhang, W.; Arias, D. H.; McCulloch, I.; Rumbles, G.; Johnson, J. C. Controlling Long-Lived Triplet Generation from Intramolecular Singlet Fission in the Solid State. *J. Phys. Chem. Lett.* **2017**, *8* (24), 6086–6091. https://doi.org/10.1021/acs.jpclett.7b02750.
(46) Kim, J.; Teo, H. T.; Hong, Y.; Oh, J.; Kim, H.; Chi, C.; Kim, D. Multiexcitonic Triplet Pair Generation in Oligoacene Dendrimers as Amorphous Solid-State Miniatures. *Angew. Chem. Int. Ed.* **2020**, *59* (47), 20956–20964. https://doi.org/10.1002/anie.202008533.
(47) Musser, A. J.; Al-Hashimi, M.; Maiuri, M.; Brida, D.; Heeney, M.; Cerullo, G.; Friend, R. H.; Clark, J. Activated Singlet Exciton Fission in a Semiconducting Polymer. *J. Am. Chem. Soc.* **2013**, *135* (34), 12747–12754. https://doi.org/10.1021/ja405427j.
(48) Sommer, M.; Huettner, S.; Thelakkat, M. Donor–Acceptor Block Copolymers for Photovoltaic Applications. *J. Mater. Chem.* **2010**, *20* (48), 10788. https://doi.org/10.1039/c0jm00665c.
(49) Stadler, R.; Auschra, C.; Beckmann, J.; Krappe, U.; Voight-Martin, I.; Leibler, L. Morphology and Thermodynamics of Symmetric Poly(A-Block-B-Block-C) Triblock Copolymers. *Macromolecules* **1995**, *28* (9), 3080–3097. https://doi.org/10.1021/ma00113a010.
(50) Hamley, I. W. *The Physics of Block Copolymers*; Oxford science publications; Oxford University Press, 1998.
(51) Heinrich, C. D.; Fischer, M.; Thurn-Albrecht, T.; Thelakkat, M. Modular Synthesis and Structure Analysis of P3HT- *b* -PPBI Donor–Acceptor Diblock Copolymers. *Macromolecules* **2018**, *51* (18), 7044–7051. https://doi.org/10.1021/acs.macromol.8b01301.

(52) Yang, C.; Lee, J. K.; Heeger, A. J.; Wudl, F. Well-Defined Donor–Acceptor Rod–Coil Diblock Copolymers Based on P3HT Containing C60: The Morphology and Role as a Surfactant in Bulk-Heterojunction Solar Cells. *J. Mater. Chem.* **2009**, *19* (30), 5416. https://doi.org/10.1039/b901732a.
(53) Guo, C.; Lin, Y.-H.; Witman, M. D.; Smith, K. A.; Wang, C.; Hexemer, A.; Strzalka, J.; Gomez, E. D.; Verduzco, R. Conjugated Block Copolymer Photovoltaics with near 3% Efficiency through Microphase Separation. *Nano Lett.* **2013**, *13* (6), 2957–2963. https://doi.org/10.1021/nl401420s.
(54) Bridges, C. R.; Yan, H.; Pollit, A. A.; Seferos, D. S. Controlled Synthesis of Fully π-Conjugated Donor–Acceptor Block Copolymers Using a Ni(II) Diimine Catalyst. *ACS Macro Lett.* **2014**, *3* (7), 671–674. https://doi.org/10.1021/mz500314p.
(55) Hollinger, J.; Seferos, D. S. Morphology Control of Selenophene–Thiophene Block Copolymers through Side Chain Engineering. *Macromolecules* **2014**, *47* (15), 5002–5009. https://doi.org/10.1021/ma501231d.
(56) Sommer, M.; Lindner, S. M.; Thelakkat, M. Microphase-Separated Donor-Acceptor Diblock Copolymers: Influence of HOMO Energy Levels and Morphology on Polymer Solar Cells. *Adv. Funct. Mater.* **2007**, *17* (9), 1493–1500. https://doi.org/10.1002/adfm.200600634.
(57) Xia, J.; Busby, E.; Sanders, S. N.; Tung, C.; Cacciuto, A.; Sfeir, M. Y.; Campos, L. M. Influence of Nanostructure on the Exciton Dynamics of Multichromophore Donor–Acceptor Block Copolymers. *ACS Nano* **2017**, *11* (5), 4593–4598. https://doi.org/10.1021/acsnano.7b00056.
(58) Zhu, L.; Tran, H.; Beyer, F. L.; Walck, S. D.; Li, X.; Ågren, H.; Killops, K. L.; Campos, L. M. Engineering Topochemical Polymerizations Using Block Copolymer Templates. *J. Am. Chem. Soc.* **2014**, *136* (38), 13381–13387. https://doi.org/10.1021/ja507318u.
(59) Sauvé, E. R.; Tonge, C. M.; Hudson, Z. M. Aggregation-Induced Energy Transfer in Color-Tunable Multiblock Bottlebrush Nanofibers. *J. Am. Chem. Soc.* **2019**, *141* (41), 16422–16431. https://doi.org/10.1021/jacs.9b08133.
(60) Merrifield, R. E. Magnetic Effects on Triplet Exciton Interactions. *Pure Appl. Chem.* **1971**, *27* (3), 481–498. https://doi.org/10.1351/pac197127030481.
(61) Parenti, K. R.; He, G.; Sanders, S. N.; Pun, A. B.; Kumarasamy, E.; Sfeir, M. Y.; Campos, L. M. Bridge Resonance Effects in Singlet Fission. *J. Phys. Chem. A* **2020**, *124* (45), 9392–9399. https://doi.org/10.1021/acs.jpca.0c08427.
(62) Burdett, J. J.; Bardeen, C. J. The Dynamics of Singlet Fission in Crystalline Tetracene and Covalent Analogs. *Acc. Chem. Res.* **2013**, *46* (6), 1312–1320. https://doi.org/10.1021/ar300191w.
(63) Kumarasamy, E.; Sanders, S. N.; Tayebjee, M. J. Y.; Asadpoordarvish, A.; Hele, T. J. H.; Fuemmeler, E. G.; Pun, A. B.; Yablon, L. M.; Low, J. Z.; Paley, D. W.; Dean, J. C.; Choi, B.; Scholes, G. D.; Steigerwald, M. L.; Ananth, N.; McCamey, D. R.; Sfeir, M. Y.; Campos, L. M. Tuning Singlet Fission in Pi-Bridge-Pi Chromophores. *J Am Chem Soc* **2017**, *139* (36), 12488–12494. https://doi.org/10.1021/jacs.7b05204.
(64) Aster, A.; Zinna, F.; Rumble, C.; Lacour, J.; Vauthey, E. Singlet Fission in a Flexible Bichromophore with Structural and Dynamic Control. *J. Am. Chem. Soc.* **2021**, *143* (5), 2361–2371. https://doi.org/10.1021/jacs.0c12384.
(65) Thompson, N. J.; Hontz, E.; Congreve, D. N.; Bahlke, M. E.; Reineke, S.; Voorhis, T. V.; Baldo, M. A. Nanostructured Singlet Fission Photovoltaics Subject to Triplet-Charge

Annihilation. *Adv. Mater.* **2014**, *26* (9), 1366–1371. https://doi.org/10.1002/adma.201304588.

(66) Yuan, D.; Niu, L.; Chen, Q.; Jia, W.; Chen, P.; Xiong, Z. The Triplet-Charge Annihilation in Copolymer-Based Organic Light Emitting Diodes: Through the "Scattering Channel" or the "Dissociation Channel"? *Phys. Chem. Chem. Phys.* **2015**, *17* (41), 27609–27614. https://doi.org/10.1039/C5CP05016B.

(67) Grieco, C.; Doucette, G. S.; Pensack, R. D.; Payne, M. M.; Rimshaw, A.; Scholes, G. D.; Anthony, J. E.; Asbury, J. B. Dynamic Exchange During Triplet Transport in Nanocrystalline TIPS-Pentacene Films. *J. Am. Chem. Soc.* **2016**, *138* (49), 16069–16080. https://doi.org/10.1021/jacs.6b10010.